iScience

CellPress
OPEN ACCESS

Article

Effect of proteins on biocementation in construction materials

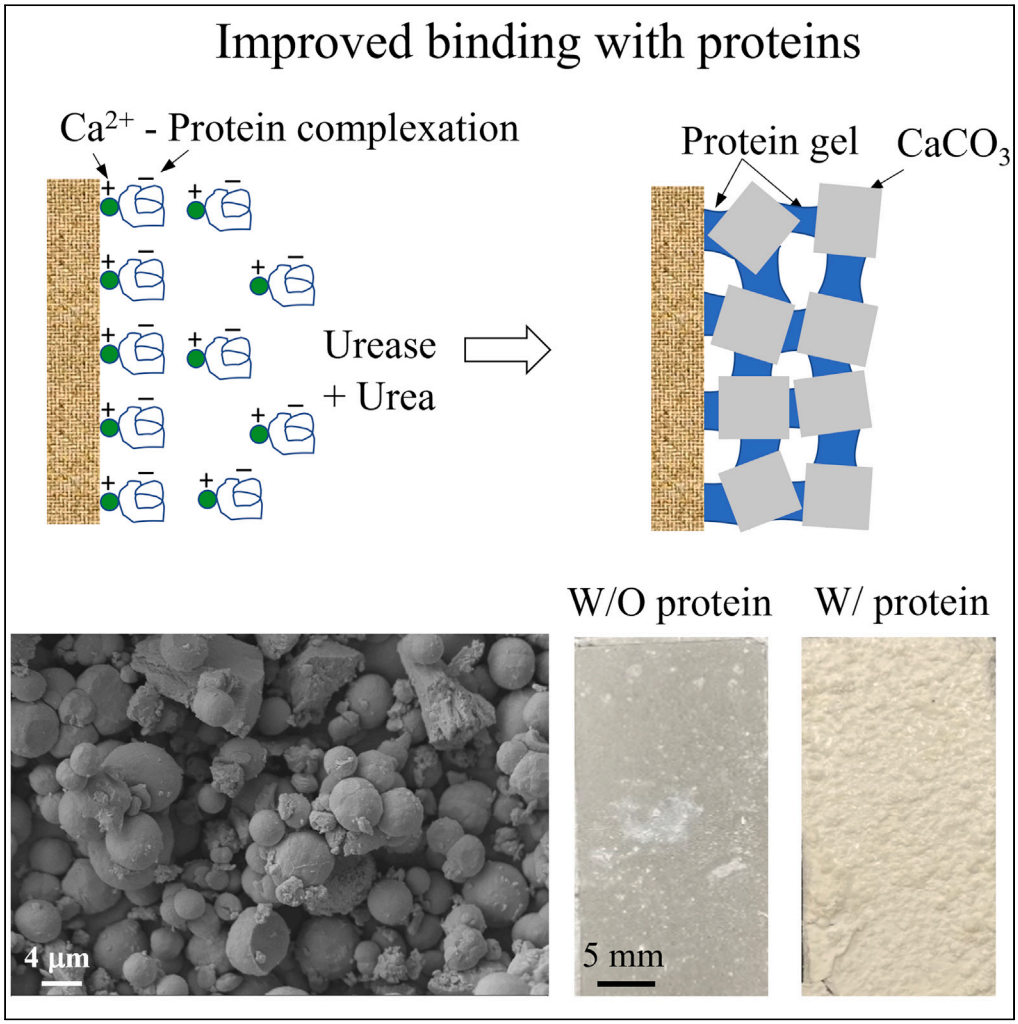

Elvis Baffoe, Edward Dauer, Ali Ghahremaninezhad

a.ghahremani@miami.edu

Highlights

Proteins enhanced the binding strength of EICP to the substrates

Proteins significantly improved the binding of EICP in cementitious environment

The pH and chemistry of solution affected the $CaCO_3$ polymorph in EICP

Baffoe et al., iScience 27, 108743
January 19, 2024
https://doi.org/10.1016/j.isci.2023.108743

iScience

CellPress
OPEN ACCESS

Article

Effect of proteins on biocementation in construction materials

Elvis Baffoe,[1] Edward Dauer,[2] and Ali Ghahremaninezhad[1,3,*]

SUMMARY

This study examines the effect of proteins on the binding property and microstructure of enzymatic-induced calcium carbonate precipitation (EICP) in cementitious environment. The protein modified precipitates generally demonstrated improved binding to a glass slide surface or cement paste surface compared to the control precipitate. A marked decrease in the amount and binding strength of the precipitates in the cementitious environment was observed due to a reduction in the urease enzyme activity. The protein modified precipitates exhibited noticeable improvement compared to the control precipitate in cementitious environment which could arise from the ability of the proteins to partially shield urease from the negative effect of high pH. The protein gel network formation due to the complexation between the proteins and Ca^{2+} provides nucleation sites for $CaCO_3$ crystallization. The FTIR, SEM, TGA, and XRD results indicated that vaterite is the dominant polymorph in cementitious environment compared to calcite in deionized water.

INTRODUCTION

Biocementation, based on the microbial- and enzyme-induced carbonate precipitation (MICP and EICP), has drawn significant attention because of lower energy consumption and more abundant raw materials. The effect of biocementation to repair cement-based materials and limestone,[1–3] to enhance the mechanical properties and permeability of porous materials,[4–7] to improve the properties of soil and sand,[4] to modify oil recovery from oil reservoirs, and to enhance bioremediation[8,9] has been studied in the past. In MICP and EICP, the urease enzymes hydrolyze urea to produce carbonate and ammonium ions. The carbonate ions react with calcium ions present in the medium to produce calcium carbonate $CaCO_3$. The primary polymorphs of $CaCO_3$ comprise amorphous calcium carbonate (ACC), vaterite, aragonite, and calcite. Formation of these polymorphs follow Ostwald's process; the ACC is first to form which then transforms to vaterite or aragonite and then finally to the stable phase calcite. Most of the $CaCO_3$ occurring naturally exhibits the calcite polymorph.[10]

The $CaCO_3$ produced using chemical synthesis usually consists of only crystalline calcite. In the case of EICP and MICP, other polymorphs including ACC, aragonite and or vaterite can also form. The marked difference between the chemical synthesis and the biological routes is that the $CaCO_3$ precipitated using the EICP or MICP method are biogenic whereas the chemically synthesized $CaCO_3$ is not. The biogenic minerals have over the years gained increasing interest due to their intricate nanostructures, superior mechanical properties, and unique functions such as support, protection, sensing, and storage.[11,12] These interesting attributes are due to the interaction between the organic molecules and inorganic constituents governing crystallization, growth, and self-assembly in the microstructure of these organic-inorganic biominerals.[13–15]

With increasing fascination for these biogenic minerals, scientists from a wide array of disciplines have been exploring the controlling factors associated with the formation of these materials and, consequently, mimicking their synthesis with the goal of fabricating advanced materials for a wide range of applications.[16] Several groups have examined the effect of biomolecules on the effects of $CaCO_3$ mineralization.[17] The polymorph and morphology of $CaCO_3$ were reported to be affected by biomolecules.[18–21] In a previous study, the role of organic molecules was indicated as the reason for the improved mechanical performance of consolidated loose sands via MICP compared to chemically synthesized $CaCO_3$, where organic molecules are not present.[22] In a recent study, the use of biomolecules was shown to improve the mechanical binding performance of loose ground hardened cement paste particles treated with EICP.[1] The adhesion of biomolecules to cracked cement paste surface and their potential to improve crack healing were investigated by Baffoe and Ghahremaninezhad.[23]

Motivated by previous studies, it is postulated that biomolecules have the potential to affect EICP processes in applications involving cementitious materials. To this end, the present study is intended to investigate the effect of different proteins, which are a type of biomolecules, on the microstructure and mechanical binding of EICP in cementitious environments. The binding property of EICP precipitate onto cement paste and silica glass surfaces was qualitatively investigated using the scratch test. Scanning electron microscopy (SEM), Fourier transform infrared spectroscopy (FTIR), thermogravimetric analysis (TGA) and X-ray diffraction (XRD) were employed to study the effect of proteins

[1]Department of Civil and Architectural Engineering, University of Miami, Coral Gables, FL 33146, USA
[2]Department of Biomedical Engineering, University of Miami, Coral Gables, FL 33146, USA
[3]Lead contact
*Correspondence: a.ghahremani@miami.edu
https://doi.org/10.1016/j.isci.2023.108743

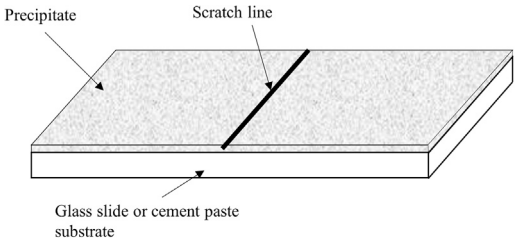

Figure 1. Schematic showing the scratch test across the precipitates

on the phase and morphology of EICP precipitates. The results from this study will shed light on the relationship between the microstructure and binding behavior of the protein modified EICP precipitates that can inform the design and engineering of biocementation for cementitious materials.

RESULTS AND DISCUSSION

Binding of precipitates to the surfaces

Glass slide-DI water

A comparison between the surfaces of the precipitates formed on glass slides in DI water before and after the scratch test as depicted in Figure 1 is shown in Figure 2. The binding of the precipitate to the glass slide surfaces was categorized as either weak, strong, or stronger. This qualitative classification is based on the amount of deformation or damage occurring in the precipitates in response to the scratching as observed from the optical images. The binding of the control precipitate and CP modified precipitate was classified as weak. The binding of NFMP and whey protein modified precipitates to the glass slide surface was classified as strong and lastly, the binding of albumin and SBI modified precipitates to glass slide surfaces was categorized as stronger. It is seen from the control and CP modified precipitates that a portion of the precipitates broke off or got detached from the glass slide after the scratch test. This demonstrates weak binding between the precipitate and the glass slide. The behavior of the control precipitate (Figure 2A) is in agreement with the observations reported in literature[24] where it was shown that precipitates without proteins were loose and detached easily from the glass slide during the scratch test. The whey protein modified precipitate shown in Figure 2D shows two scratch stripes, but precipitates were strongly adhered to the glass slide and did not detach. The albumin modified precipitates (Figure 2E) show stronger cohesion and strongly adhered onto the glass slide. This was revealed by a faint scratch line on the precipitate.

It is seen from the NFMP modified precipitates (Figure 2C) that a large amount of precipitates covered the glass slide, and the precipitates were seen to be cohesive among the precipitates. The NFMP modified precipitate did not show any noticeable scratching after testing. This could be attributed to the strong adhesion of the NFMP modified precipitate to the glass slide. This result is consistent with the observations made by Martin et al.[24] Proteins have a negative charge in the EICP solution and can bind to the negatively charged glass slide surface via Ca^{2+} bridging. The proteins can facilitate the formation of a gel network through complexation with Ca^{2+},[25,26] which serves nucleation sites for EICP precipitation and provides adhesion at the substrate surface/precipitate interface as well as cohesion within the precipitate.

The SBI modified precipitate showed no detachment or surface scratch after the scratch test. It is interesting to note that among all the samples tested, the SBI modified precipitate showed the greatest adhesion to the glass slide surfaces after the scratch test. It is worth noting that the whey protein, albumin, NFMP and SBI modified precipitates showed better interparticle cohesion compared to the control precipitate and the CP modified precipitate.

Glass slide-Cement pore solution

Figure 3 illustrates a comparison between the surfaces of the precipitates formed on glass slides in the cement pore solution before and after the scratch test. The binding of the control precipitate and CP modified precipitate to the glass slide surfaces was classified as very weak because precipitates detached easily during scratching. The binding of the SBI modified precipitate to glass slide surface was classified as weak and lastly, the binding of the albumin, NFMP and whey modified precipitates to glass slides was categorized as strong. As shown in Figures 3D–3F, NFMP, whey protein and albumin, modified precipitates, respectively, showed a larger amount of precipitates on the glass slide. The adsorption and adhesive property of these proteins (NFMP, whey protein and albumin) contributed to the stronger adhesion of the precipitates to the glass slide.

It is noted that overall, the amount of the EICP precipitates in the cement pore solution is lower than in the DI water. This is attributed to the reduction in urease activity which is caused by the irreversible inactivation of the urease enzyme in the high pH (~12.5) environment.[27] Comparing the control precipitates to the protein modified precipitates, it is apparent that the proteins assisted in protecting urease against inactivation in the high pH condition[28] as the protein modified precipitates exhibited higher amount of precipitate compared to the control precipitate.

The reduced binding strength of the protein modified precipitates in the cement pore solution compared to in the DI water is noted and this is more pronounced in the case of the SBI modified precipitate as seen in Figures 2F and 3C. This can be attributed to the extent of denaturation of the proteins due to the combined effect of high pH and urea.[1] Both urea and high pH of a solution are known denaturation factors,

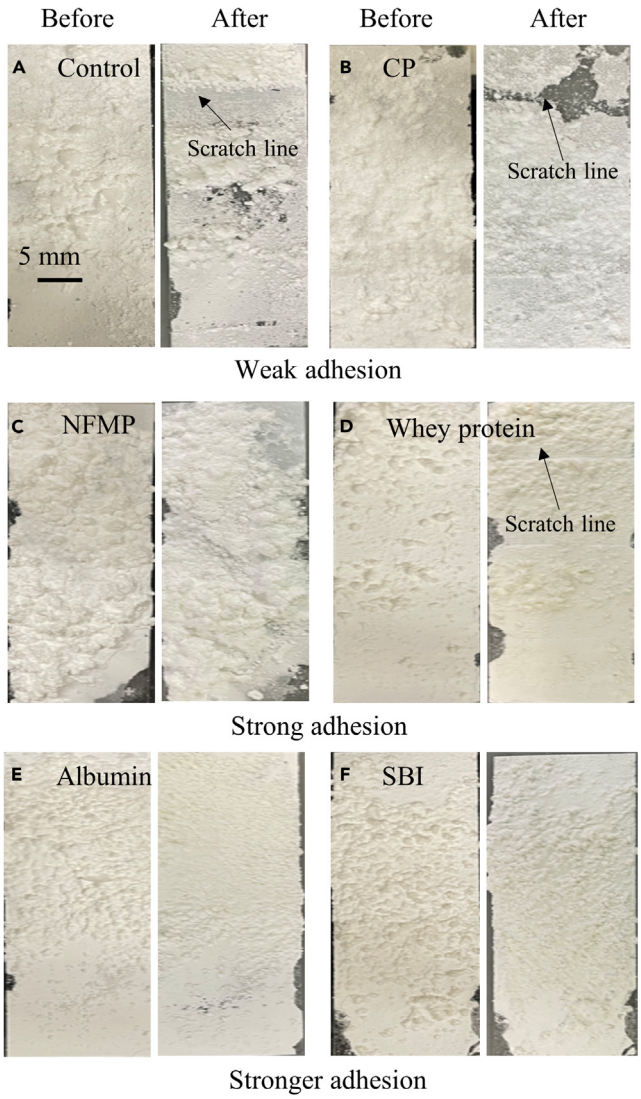

Figure 2. Images of the precipitates on glass slides in DI water before and after the scratch test
Corresponding to (A) control, (B) CP, (C) NFMP, (D) whey protein, (E) albumin, and (F) SBI.

which break intermolecular bonds in the molecular structure of the proteins impacting their properties.[29] The combined effect of these denaturation factors reduces the binding strength of the protein modified precipitates to the glass slide.

Cement paste-DI water

Figure 4 shows a comparison between the precipitates formed on cement paste surface in DI water before and after scratch test. The overall pH of the solution after the reaction was approximately 9.6. The increase in the pH of the solution is due to the dissolution of ions, including Na^+, K^+, and Ca^{2+} from the cement paste surface into the solution. The control sample showed no precipitate on the surface of the cement paste so only one image is shown in Figure 4A. The binding of the albumin and CP modified precipitates to the cement paste surface was very weak compared to the rest of the protein modified precipitates. The whey protein modified precipitates showed more precipitate on the surface of the cement paste surface and a stronger adhesion compared to the albumin and CP modified precipitates. The SBI and NFMP modified precipitates showed greater deposition on the surface of the cement paste surface and were classified as stronger. Interestingly, the SBI modified precipitates showed the strongest adhesion to the cement paste surface among the precipitates. Comparing the SBI modified precipitates in different conditions, as shown in Figures 2F, 3C, and 4E, clearly indicates that the adhesion of the SBI modified precipitates is deteriorated when the pH of the bulk solution is increased to a level of about 12.5 in the presence of urea.

According to literature, the binding of proteins or amino acids onto $CaCO_3$ may lead to the formation of organic-inorganic composites. Such materials have been noted to possess enhanced mechanical property.[30,31] The glass slide utilized in the experiment is positively charged

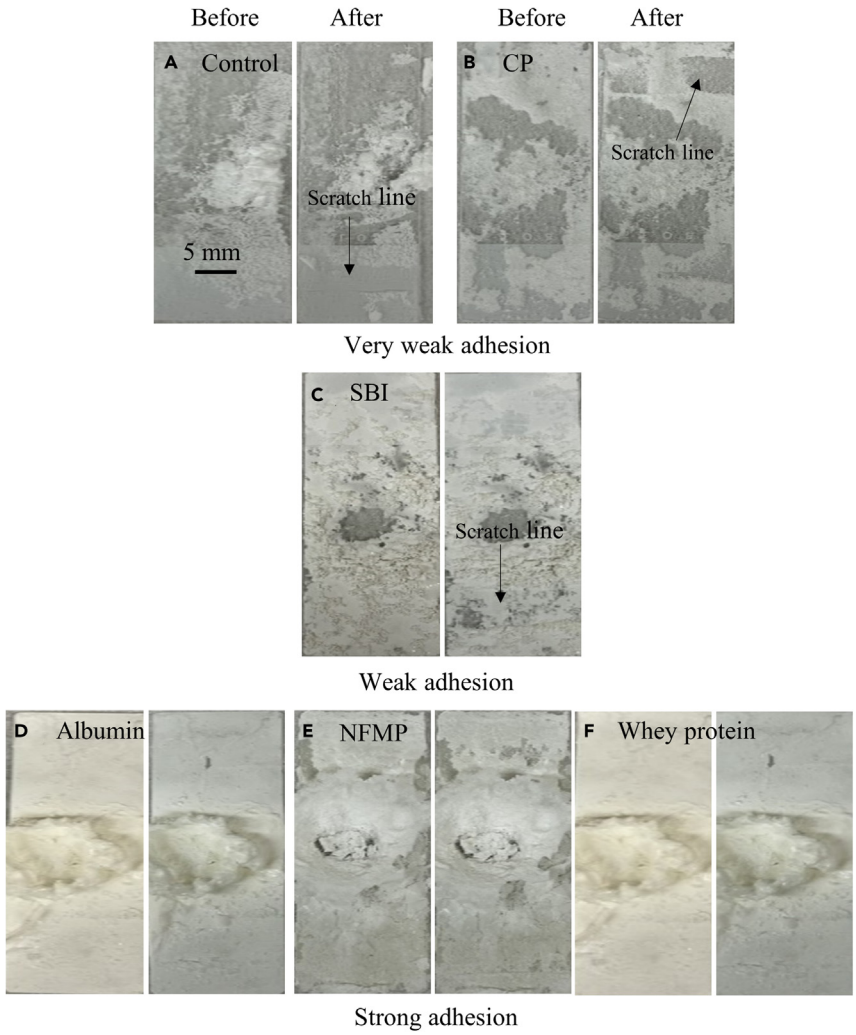

Figure 3. Images of the precipitates on glass slides in cement pore solution before and after the scratch test
Corresponding to (A) control, (B) CP, (C) SBI, (D) albumin, (E) NFMP, and (F) whey protein.

when unused, however, as urea hydrolyzes during the precipitation process, the glass slide becomes negatively charged due to increased pH.[32,33] The surface of cement paste is heterogeneously charged.[1] At the same time, due to the deprotonation of the amino functional groups in proteins at high pH, the proteins becomes highly negatively charged.[1] In this situation, the negatively charged proteins adsorbed onto the negatively charged glass slide and heterogeneously charged cement paste surface through Ca^{2+} bridging.[1,34] In addition the interaction between Ca^{2+} and the charged proteins can lead to formation of crosslinked networks which can increase the interparticle binding of the precipitates and also enhance the binding between the precipitates and the deposition surfaces.[1] The observed low binding strength of the CP-modified precipitate can be attributed to the low adsorption of the CP molecule onto the glass slide or cement paste surface and the low adhesive property of the CP molecule.[23] A schematic illustrating the adhesive and cohesive bonding provided by the proteins is shown in Figure 5. Table 1 summarizes the binding strength comparisons among the precipitates in the different conditions. It is to be noted that the protein gel network formation and binding forces are dependent on the molecular structure of the proteins. Further theoretical and computational studies could provide additional insights into the relationships between the molecular structure and binding force of the proteins.

FTIR

Glass slide-DI water

The FTIR spectra shown in Figure 6A exhibit relatively sharp peaks located at 712 cm^{-1} and 872 cm^{-1} for the control precipitate and the protein modified precipitates, indicating the presence of the calcite polymorph of $CaCO_3$.[35] The peaks located at 745 cm^{-1} and 1087 cm^{-1} are assigned to the formation of the vaterite polymorph in the precipitates.[36] These peaks were more intense in the NFMP and SBI modified

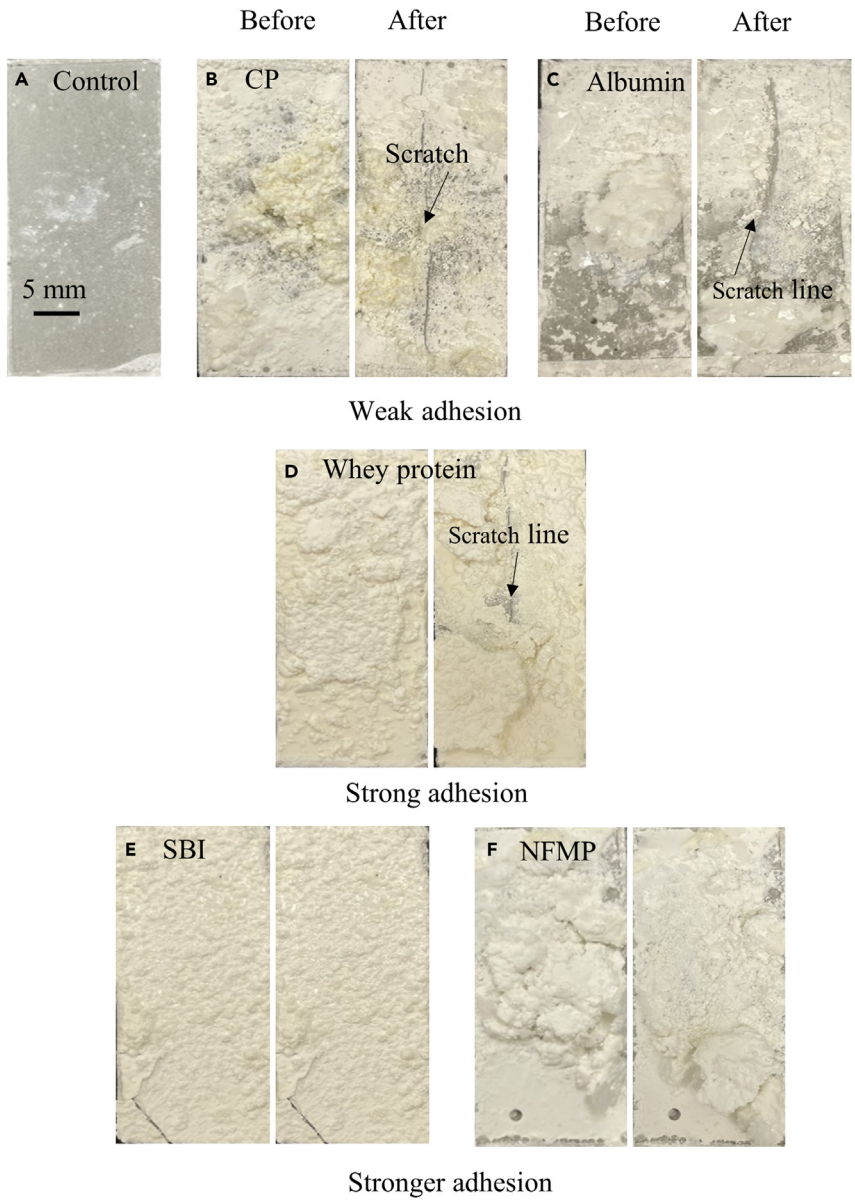

Figure 4. Images of the precipitates on cement paste surface in DI water before and after the scratch test
Corresponding to (A) control, (B) CP, (C) albumin, (D) whey protein, (E) SBI, and (F) NFMP.

precipitates than that of the control precipitate. This indicates that NFMP and SBI were more effective in stabilizing vaterite. The characteristic peaks located at 1640 cm^{-1} in the protein modified precipitates mostly provide information about the presence of water or amide I of the amino acids present in the proteins.[35,37] For -OH peak, there should be a corresponding broad peak in the range of 3100 cm^{-1}-3400 cm^{-1}.[35] Since the -OH peak located within the range of 3100 cm^{-1}-3400 cm^{-1} is absent or weak, the peak at 1640 cm^{-1} is likely to be attributed to the presence of amide I due to the presence of protein.[37,38] It was noticed that the whey protein, albumin and CP modified precipitates showed weak or no peak corresponding to vaterite. Interestingly, the peaks corresponding to calcite for these precipitates were sharper than that of the control precipitate, providing an indication that calcite was more dominant among the $CaCO_3$ polymorphs present in these samples. The peak at 1797 cm^{-1} reveals the high content of $CaCO_3$.[23] The characteristic peaks located at 2811 cm^{-1} for the CP modified precipitates and ranging between 3044 cm^{-1} and 3127 cm^{-1} for the control precipitates and CP modified precipitates may be assigned to the stretching vibration of the C-H group of biomolecules (protein and urea) which is positioned in the aliphatic hydrophobic side chain of the biomolecules.[39] The asymmetric band located at 1400 cm^{-1} is attributed to the presence of vaterites in the microstructure of the precipitates.[40]

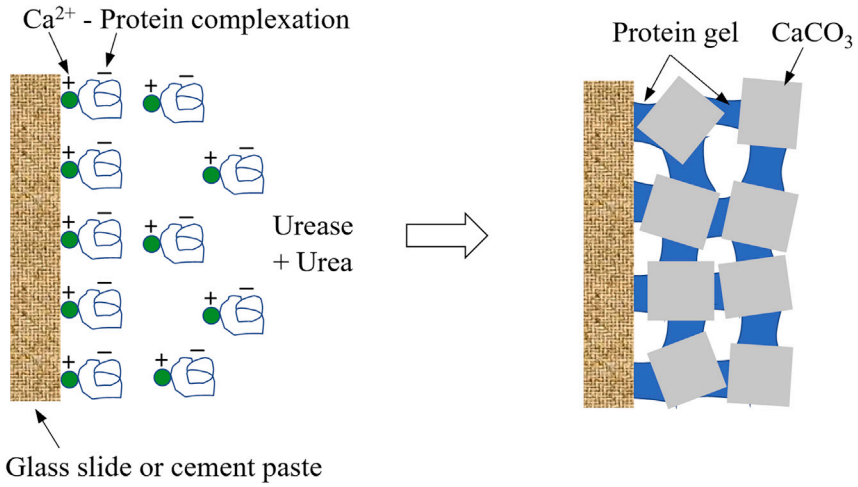

Figure 5. Schematic illustrating binding provided by the proteins at the solid surface/$CaCO_3$ interface (adhesion) and at the $CaCO_3$/$CaCO_3$ interface (cohesion)

Glass slide-Cement pore solution

The FTIR spectra of the precipitates formed on glass slides in cement pore solution are illustrated in Figure 6B. It can be seen that the peaks corresponding to vaterite were dominant in the control precipitates, whey protein and albumin modified precipitates. The spectrum of the control precipitate appeared differently from that of the other samples shown in this figure. The activity of the urease enzyme is affected by the pH level of the environment.[27] The optimum pH range for a full urease activity is reported to be within 8–12.[27] Beyond the pH level of 12, the activity of urease enzyme is expected to be reduced.[27] This is because the urease enzyme, when exposed to pH levels beyond 12, denatures due to the disruption of the ionic and hydrogen bonds required to maintain the active conformation of the proteinaceous enzyme.[27] Since the pH level of the pore solution was above 12, the activity of the urease enzyme is expected to be affected reducing the precipitation reaction. The addition of the proteins could provide sites for the interaction with the urease enzymes and prevent the urease from excessive denaturation at high pH. That is why, compared to the control precipitate, the precipitates modified with proteins showed peaks that were more characteristic of $CaCO_3$.

It is observed that the precipitates formed in the cement pore solution tend to comprise more vaterite polymorph compared to the precipitates formed in DI water. It has been reported that increased pH has negligible effect on the stabilization of vaterite polymorph.[41–43] The crystallization of the $CaCO_3$ polymorphs has been shown to be influenced by the presence of ions in the precipitating medium.[41,42,44] For instance, House et al.,[45] Song et al.,[42] and Bischoff et al.,[46] reported that ionic particles such as Mg^{2+}, SO_4^{-2}, NH_4^+ and PO_4^{-3} inhibit calcite recrystallization. These ions interact with organic molecules and adsorb onto crystal faces. As they are adsorbed onto the crystal faces, calcite nucleation and growth are altered due to inhibition by the complexes.[44] According to the "Ostwald step rule" metastable vaterites are initially formed during the $CaCO_3$ reaction process.[41] Depending on the concentration of ions in the pore solution, it is plausible that these ions inhibited the crystallization of calcites and that was indicated by the sharper peak corresponding to vaterite in Figure 6B than Figure 6A. Another possibility for the increased formation of vaterite could be the change in the molecular structure and physicochemical properties including surface charge of the proteins in the high pH environment of the cement pore solution as indicated in our and other researchers' prior investigations.[1,47] Thus, it can be stipulated that the increase in charge of the proteins at high pH could potentially increase the interaction between the proteins and vaterite crystals stabilizing this polymorph and inhibiting its conversion to calcite. The –OH peak at 3353 cm^{-1} showed a bulky peak and this was because after the oven-drying process, the control precipitate still had some moisture. The characteristic peaks ranging between 3044 cm^{-1} and 3127 cm^{-1} for the precipitates may be assigned to the stretching vibration of the C-H group of biomolecules (protein and urea).[39]

Table 1. Summary of the binding strength of the precipitates

Sample	Control	Whey protein	Albumin	NFMP	SBI	CP
Glass slide-DI water	Weak	Strong	Stronger	Strong	Stronger	Weak
Glass slide-Cement pore solution	Very weak	Strong	Strong	Strong	Weak	Very weak
Cement paste-DI water	No precipitate	Strong	Weak	Stronger	Stronger	Very weak

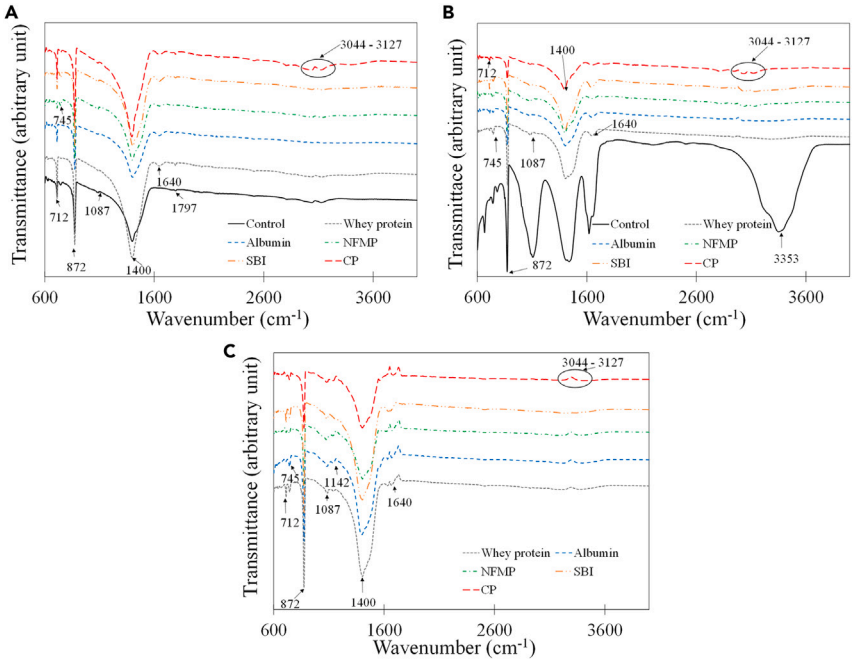

Figure 6. FTIR results

Spectra of the precipitates formed on glass slides in (A) DI water and (B) cement pore solution and (C) on cement paste surface in DI water.

Cement paste-DI water

The FTIR spectra of the precipitates formed on cement paste surface shown in Figure 6C revealed the typical peaks of $CaCO_3$ corresponding to calcite at 872 cm^{-1} and 1400 cm^{-1}.[35] As shown in Figure 4A, the control precipitate showed no deposition on the surface of the cement paste, hence the surface of the paste was not scratched for FTIR analysis. Interestingly, it can be observed that the protein modified precipitates showed marked peaks corresponding to vaterites. Comparing Figures 6A and 6C, the increase in the vaterite formation in the precipitate formed on the surface of the cement paste in DI water compared to the glass slide in DI water, can be attributed to increased pH and ionic strength locally near the cement paste surface. Ions are dissolved into the solution near the surface of the cement paste as a result of continued hydration of unhydrated cement particles located on the surface and diffusion of ions from the interior of the cement paste.[48] The presence of ions locally near the cement paste surface is likely to interfere with the crystallization by adsorbing onto vaterite crystals and stabilizing them.

SEM

Glass slide-DI water

Figure 7 shows the SEM images of the precipitates formed on glass slides in DI water. It is seen that the dominant polymorph in the control precipitate was calcite. These calcites exhibited rhombohedral and cubic shapes. The SEM image of the whey protein modified precipitate shown in Figure 7B exhibited calcite with the presence of some isolated vaterites. This is consistent with the FTIR results discussed in Figure 6A. The SEM of the albumin modified precipitate is shown in Figure 7C. In the albumin modified precipitates, calcite appears to be the main polymorph with the sporadic presence of vaterite. The size of the vaterite polymorph was in the range of ~5 μm while the calcite exhibited varying sizes. The SEM image of the NFMP modified precipitate showed a mix of calcite and vaterite demonstrating that NFMP was effective in stabilizing vaterite polymorph. The SBI modified precipitate also showed a mix of vaterite and calcite. The microstructure of the CP modified precipitates shown in Figure 7F consisted mainly of calcite but had some isolated large sizes of vaterite. The morphology of the calcites in the CP modified precipitates was similar to that of the control precipitate.

The adsorption of the proteins onto surfaces is highly influenced by the charge density of the protein as discussed in the previous studies.[1,49] The presence of organic molecules in the reaction medium increases the supersaturation of the precipitation solution leading to the formation of vaterites with smaller sizes.[50,51] On textural differences among the vaterites in the samples, the vaterites in the CP modified precipitates exhibited smoother texture compared to the rough texture of vaterites in the albumin, NFMP and SBI modified precipitates. This difference is attributed to the specific interactions between vaterite and each protein.[52] A summary of the SEM observations regarding the polymorphs formed on glass slides in DI water is shown in Table 2.

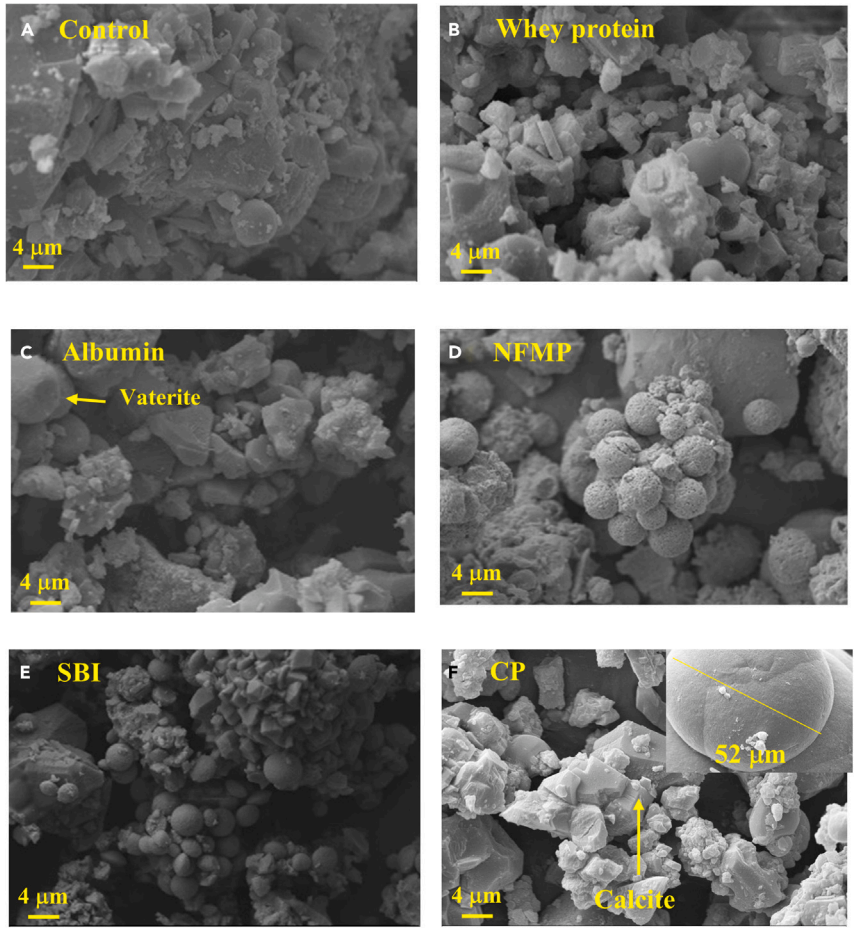

Figure 7. SEM images of the precipitates formed on glass slides in DI water
Corresponding to (A) control, (B) whey protein, (C) albumin, (D) NFMP, (E) SBI, and (F) CP.

Glass slide-Cement pore solution

Figure 8 shows the SEM images of the precipitates deposited on glass slides in cement pore solution. The microstructure of the control precipitate showed some fiber-like features and some spherical shaped phases which are likely to be vaterites based on the results of the FTIR shown in Figure 6B. These fiber-like features do not resemble typical polymorphs seen in EICP. The presence of these fiber-like phases may be a result of the reduced activity of the urease enzymes due to the higher pH level of the pore solution as evidenced in Figures 3A and 6B.

Shown in Figures 8B and 8C, are the microstructure features of the precipitates modified with whey protein and albumin in cement pore solution. It can be seen that the dominant polymorph in these precipitates are vaterites. The vaterites in the whey protein modified precipitate appeared smaller in size than the vaterites in the albumin modified precipitates possibly due to the adsorption variations and conformational differences of the proteins[53] in the cement pore solution. The textural characteristics were however similar in both cases. Porous vaterites appeared to be dominant in the NFMP modified precipitate similar to what occurred in Figure 7D. The SEM image of the SBI modified precipitate showed vaterite with sporadic presence of calcite. Similar to the control precipitate, the microstructure of the CP modified precipitate

Table 2. Summary of the SEM observations of the precipitates in the three different conditions

Sample	Control	Whey protein	Albumin	NFMP	SBI	CP
Glass slide-DI water	Calcite	Calcite	Calcite-sporadic vaterite	Calcite-vaterite	Calcite-vaterite	Calcite-sporadic vaterite
Glass slide-Cement pore solution	Some vaterite	Vaterite	Vaterite	Vaterite	Vaterite-sporadic calcite	Some vaterite
Cement paste-DI water	No precipitate	Calcite-vaterite	Vaterite-sporadic calcite	Vaterite	Calcite-vaterite	Vaterite-sporadic calcite

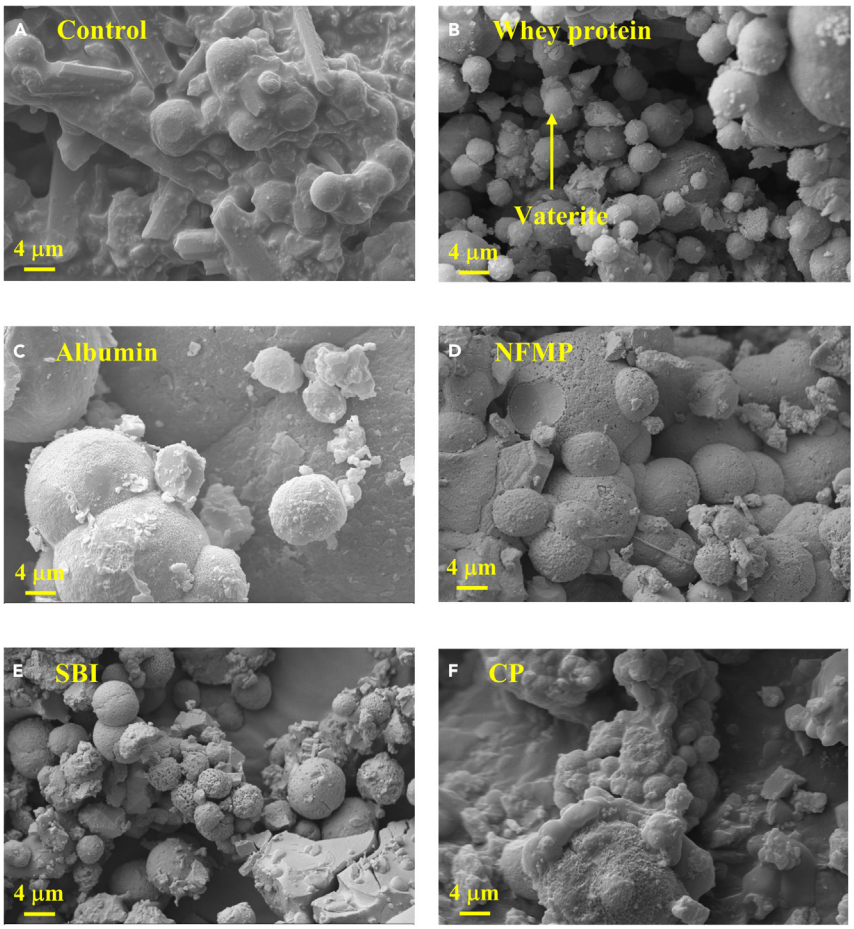

Figure 8. SEM images of the precipitates formed on glass slides in cement pore solution
Corresponding to (A) control, (B) whey protein, (C) albumin, (D) NFMP, (E) SBI, and (F) CP.

appears to contain some vaterite. It should be noted that both the control and CP modified precipitates in cement pore solution showed a small amount of precipitate and with very weak binding. A summary of the polymorphs formed on glass slides in cement pore solution is shown in Table 2.

Cement paste-DI water

The SEM of the protein modified precipitates deposited on cement paste surface in DI water is shown in Figure 9. It should be emphasized that the control precipitate did not show any deposition on the cement paste surface hence SEM images could not be obtained for this sample. It is noted that vaterite appears to be a primary polymorph in all the protein modified precipitate on cement paste. Calcite is also seen to different degrees in the precipitates. This observation is in good agreement with the FTIR results discussed previously. The increase in the formation of vaterite in the precipitates on cement paste in DI water compared to that on the glass slide in DI water is due to higher local pH and ionic concentrations near the cement paste. The increased interaction between the proteins and vaterite crystal surface in high pH as well as the adsorption of ions present in the medium onto vaterite crystal surface can stabilize vaterite and inhibit the transformation of vaterite to calcite.[41,42] A summary of the SEM observations of the $CaCO_3$ polymorphs in the precipitates on cement paste surface in DI water is included in Table 2. The SEM and FTIR results do not indicate a noticeable presence of ACC in the precipitates. No strong relationships can be observed from a comparison between binding strength and phase composition, as provided in Tables 1 and 2. This suggests the more important role the adhesive properties of proteins play in the binding strength of the precipitates.

TG/DTG

Figure 10 illustrates the TG/DTG curves of the precipitates corresponding to the three different conditions. Figures 10A–10F represent the TG/DTG results of the control, whey protein, albumin, NFMP, SBI and CP modified precipitates, respectively. The precipitates showed similar decomposition peaks, so the general peak ranges of the precipitates were used in the analysis.

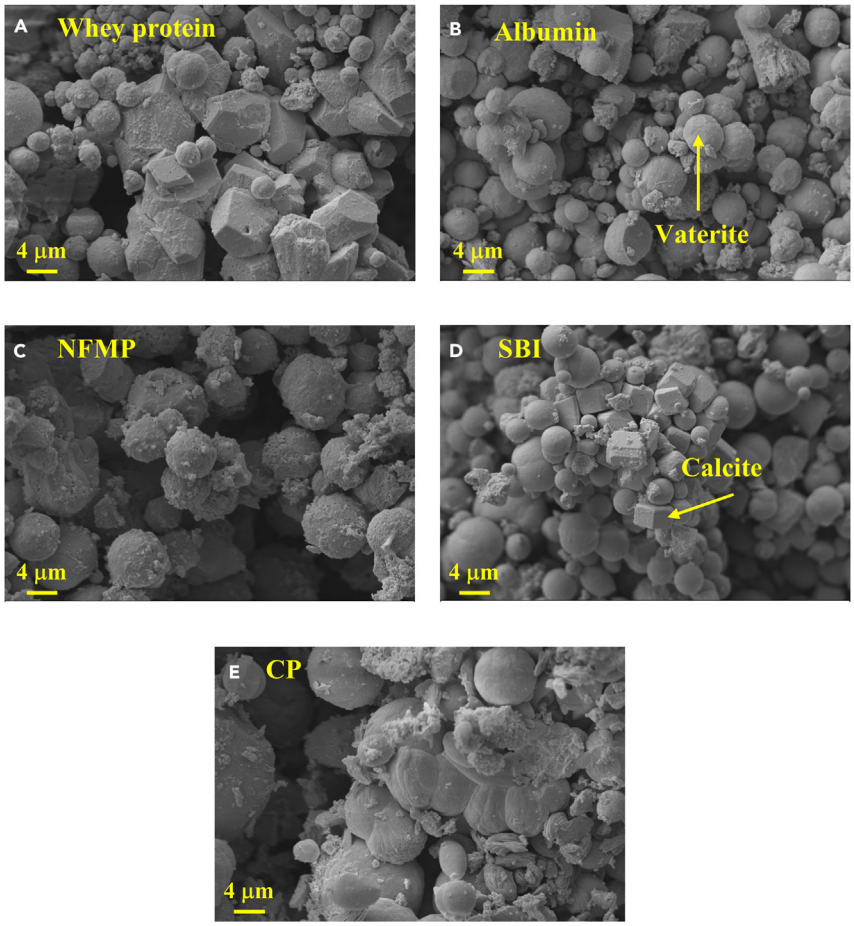

Figure 9. SEM images of the precipitates formed on cement paste surface in DI water
Corresponding to (A) whey protein, (B) albumin, (C) NFMP, (D) SBI, and (E) CP.

The mass loss that occurred between 200ºC and 280ºC corresponds to the decomposition of urea and protein.[1,54] The gradual mass loss that occurred between 300ºC and 580ºC can be attributed to the decomposition of the poorly crystalline or metastable phases of $CaCO_3$.[49,55] The metastable phases consist of vaterites based on the FTIR and SEM results, discussed previously. It can be noticed that this gradual decomposition was more noticeable in the protein modified precipitates. Moreover, it is observed that the precipitates formed on glass slide in cement pore solution and on cement paste in DI water showed noticeable mass loss in this temperature range. This is in support of the FTIR and SEM results showing increased presence of vaterite in these precipitates. It is seen that a mass loss occurred at the temperature ranging between 600ºC and 780ºC for the protein modified precipitates and between 600ºC and 800ºC for the control precipitate. This mass loss is attributed to the decomposition of calcites.[1,56] The peak corresponding to this mass loss for the protein modified precipitates occurred at a slightly lower temperature compared to the control precipitate; such variation in the decomposition temperature may be due to the presence of vaterites and smaller crystals of calcites.

In the case of the CP modified precipitate on the glass slide in DI water shown in Figure 10F, the weak gradual mass loss within the temperature range of 300ºC and 580ºC was similar to what occurred in the control precipitate in 10a and interestingly the SEM of these two samples showed only calcites as the primary polymorph. This may provide an indication that CP in this condition did not favor vaterite formation possibly due to the lower interaction between CP and vaterite. Using the TGA results, the difference in the calcium carbonate content of the protein modified precipitates and the control precipitate on the glass slide in DI water was quantified to be in the range of 5–9%, which can be attributed to the content of protein gel in the protein modified precipitates.

XRD

The XRD results of the precipitates are shown in Figure 11. For the precipitates formed on glass slides in DI water (Figure 11A), it is seen that the dominant polymorph among all the precipitates was calcite; CP exhibited the highest calcite peak, indicating a relatively large content of the calcite polymorph in the microstructure of the CP modified precipitates as demonstrated in the FTIR, SEM, and TGA results. It is also shown that the peaks corresponding to vaterite were dominant in some protein modified precipitates, especially those modified with NFMP and SBI.

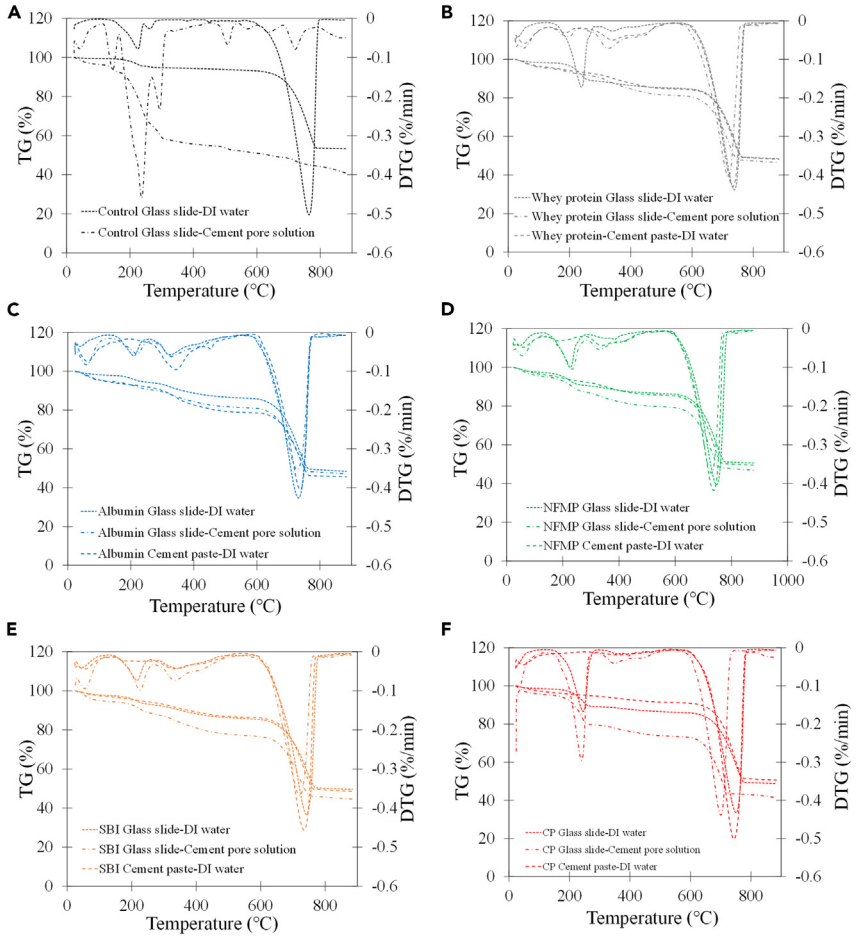

Figure 10. TGA analysis

TG/DTG results of the (A) control, (B) whey protein, (C) albumin, (D) NFMP, (E) SBI and (F) CP modified precipitates, respectively.

For the precipitates formed on glass slide in cement pore solution (Figure 11C), it is seen that the calcite peaks were not intense compared to the precipitates formed on glass slide in DI water as supported by the FTIR, SEM, and TGA results. The peaks corresponding to vaterite exhibited a higher intensity for the whey protein, albumin and NFMP modified precipitates compared to their respective counterparts formed on glass slide in DI water shown in Figure 11A. The weak peaks associated with the control precipitate and CP modified precipitate demonstrate very low enzymatic activity and calcium carbonate precipitation as a result of the high pH.

Figure 11E shows the XRD spectra of the precipitates formed on the cement paste surface in DI water. As discussed before, the control precipitate showed no deposition on the cement paste surface, hence the XRD spectrum for the control precipitate could not be obtained. Vaterite appeared dominant in the case of all protein modified precipitates except in the SBI modified precipitate where a mix of calcite and vaterite is observed. It is noticed that a peak corresponding to aragonite appeared in the XRD spectra, which was conspicuously missing in the FTIR and SEM results shown in Figures 6C and 9. The inability of the FTIR and SEM to capture the aragonite peaks may be due to the relatively small amount of this polymorph in the precipitates.

The phase proportions of the precipitates obtained using the Rietveld refinement are depicted in Figures 11B, 11D and 11F. Calcite polymorph dominated the precipitates deposited on the glass slides in DI water. On glass slides in cement pore solution, it is noticed that vaterite was the dominant polymorph in most of the precipitates. Consistent with what has been discussed, precipitates on the cement paste surface in DI water showed the formation of a large amount of vaterite. It is worth noting that SBI tends to favor calcite formation in all three experimental conditions as evident from Figures 11B, 11D, and 11F.

Conclusions

The effect of proteins on the EICP precipitation process in three different conditions was investigated in this paper. The following conclusions can be drawn from the results of this study.

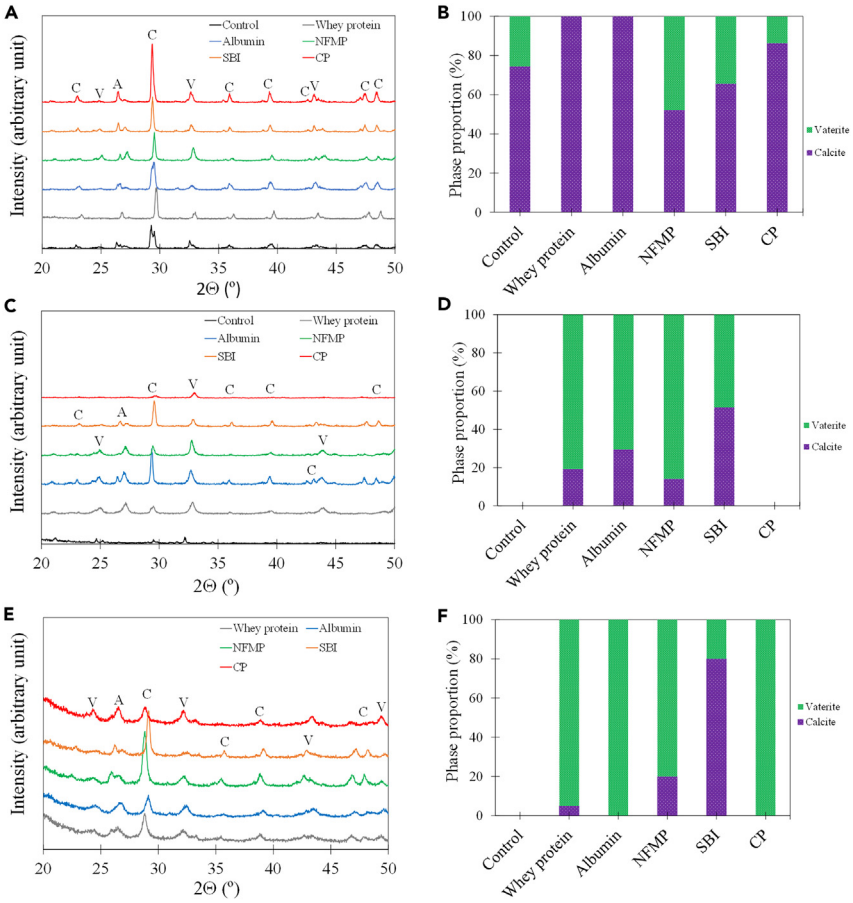

Figure 11. XRD analysis

XRD spectra and crystalline phase quantification of the precipitates formed on, (A) and (B) glass slide in DI water, (C) and (D) glass slide in cement pore solution and, (E) and (F) cement paste in DI water. A = Aragonite, V=Vaterite and C=Calcite.

- The protein modified precipitates showed improved binding to the glass slide surface in DI water compared to the control precipitate. In cement Pore solution, the control precipitate showed a lower amount and very weak binding to the glass slide surface possibly due to the reduced enzymatic activity in the high pH of the cement pore solution. Interestingly, the protein modified precipitates generally demonstrated increased amount and improved binding compared to the control precipitate in cement pore solution. The proteins appeared to protect the urease against degradation at high pH. While the control precipitate showed insignificant binding to the cement paste surface, the protein modified precipitate demonstrated significant binding to the cement paste surface. The proteins can improve binding at the $CaCO_3$/substrate interface (adhesion) and $CaCO_3$/$CaCO_3$ interface (cohesion) due to a gel network formation as a result of complex formation with Ca^{2+}.
- The FTIR, SEM, TGA, and SEM examinations indicated that vaterite is more favorable polymorph of $CaCO_3$ in the protein modified precipitates at high pH and ionic strength. The increased interaction between the proteins and vaterite crystal surface and the adsorption of the proteins onto vaterite crystal surface during the crystallization process can stabilize vaterite and inhibit its transformation to calcite. However, SBI modified precipitate showed a relatively noticeable amount of calcite in all different conditions studied here.

The results from this study provide valuable insight into the microstructure-property relationships in the protein modified EICP precipitation that can assist in developing enhanced biocementation in the construction material applications.

Limitations of the study

The effect of protein concentration on the binding and microstructure of the EICP precipitates needs to be further examined. The nanoscale adhesion testing is needed to provide quantitative values of the binding strength at the nanoscale.

STAR★METHODS

Detailed methods are provided in the online version of this paper and include the following:

- KEY RESOURCES TABLE
- RESOURCE AVAILABILITY
  - Lead contact
  - Materials availability
  - Data and code availability
- METHOD DETAILS
  - Materials
  - Material characterization

ACKNOWLEDGMENTS

This study was supported in part by the National Science Foundation under the CAREER award number 1846984 and the Office of Naval Research under the Award Number N00014221255. Any opinions, findings, and conclusions or recommendations expressed in this material are those of the author(s) and do not necessarily reflect the views of the National Science Foundation.

AUTHOR CONTRIBUTIONS

A.G. and E.B. designed and coordinated the study. E.B. prepared the samples and characterized the precipitates. E.B. and A.G. cowrote the paper. E.B., A.G., and E.D. discussed the results and commented on the manuscript. A.G. supervised the study.

DECLARATION OF INTERESTS

The authors declare no competing interests.

Received: August 8, 2023
Revised: October 7, 2023
Accepted: December 12, 2023
Published: December 14, 2023

REFERENCES

1. Baffoe, E., and Ghahremaninezhad, A. (2022). The effect of biomolecules on enzyme-induced calcium carbonate precipitation in cementitious materials. Construct. Build. Mater. *345*, 3.
2. Chunxiang, Q., Jianyun, W., Ruixing, W., and Liang, C. (2009). Corrosion protection of cement-based building materials by surface deposition of CaCO3 by Bacillus pasteurii. Mater. Sci. Eng. C *29*, 1273–1280.
3. De Muynck, W., Verbeken, K., De Belie, N., and Verstraete, W. (2010). Influence of urea and calcium dosage on the effectiveness of bacterially induced carbonate precipitation on limestone. Ecol. Eng. *36*, 99–111.
4. Whiffin, V.S., van Paassen, L.A., and Harkes, M.P. (2007). Microbial carbonate precipitation as a soil improvement technique. Geomicrobiol. J. *24*, 417–423.
5. DeJong, J.T., Fritzges, M.B., and Nüsslein, K. (2006). Microbially Induced Cementation to Control Sand Response to Undrained Shear. J. Geotech. Geoenviron. Eng. *132*, 1381–1392.
6. DeJong, J.T., Mortensen, B.M., Martinez, B.C., and Nelson, D.C. (2010). Bio-mediated soil improvement. Ecol. Eng. *36*, 197–210.
7. Ivanov, V., and Chu, J. (2008). Applications of microorganisms to geotechnical engineering for bioclogging and biocementation of soil *in situ*. Rev. Environ. Sci. Biotechnol. *7*, 139–153.
8. Ferris, F.G., Phoenix, V., Fujita, Y., and Smith, R.W. (2004). Kinetics of calcite precipitation induced by ureolytic bacteria at 10 to 20°C in artificial groundwater. Geochem. Cosmochim. Acta *68*, 1701–1710.
9. Chaturvedi, S., Chandra, R., and Rai, V. (2006). Isolation and characterization of Phragmites australis (L.) rhizosphere bacteria from contaminated site for bioremediation of colored distillery effluent. Ecol. Eng. *27*, 202–207.
10. Polowczyk, I., Bastrzyk, A., and Fiedot, M. (2016). Protein-mediated precipitation of calcium carbonate. Materials *9*, 944.
11. Lowenstam, H.A., and Weiner, S. (1989). On Biomineralization (Oxford University Press).
12. Talham, D.R. (2002). Biomineralization: Principles and Concepts in Bioinorganic Materials Chemistry Stephen Mann*2* (Oxford University Press), p. 675. New York, 2001. Cryst Growth Des.
13. Kamali, M., and Ghahremaninezhad, A. (2018). Effect of biomolecules on the nanostructure and nanomechanical property of calcium-silicate-hydrate. Sci. Rep. *8*, 9491.
14. Baffoe, E. (2023). Effect of Biomolecules on the Self-Healing and Carbonation Curing of Infrastructure Materials.
15. Wehbe, Y. (2016). Bio-inspired Self-Healing Infrastructure Materials.
16. Wang, X., Kong, R., Pan, X., Xu, H., Xia, D., Shan, H., and Lu, J.R. (2009). Role of ovalbumin in the stabilization of metastable vaterite in calcium carbonate biomineralization. J. Phys. Chem. B *113*, 8975–8982.
17. Briegel, C., Coelfen, H., and Seto, J. (2012). Single amino acids as additives modulating CaCO3 mineralization. Adv. Top. Biomineralization *33*. E7–A85.
18. Guo, X.H., and Yu, S.H. (2007). Controlled mineralization of barium carbonate mesocrystals in a mixed solvent and at the air/solution interface using a double hydrophilic block copolymer as a crystal modifier. Cryst. Growth Des. *7*, 354–359.
19. Hwang, E.T., Tatavarty, R., Chung, J., and Gu, M.B. (2013). New functional amorphous calcium phosphate nanocomposites by enzyme-assisted biomineralization. ACS Appl. Mater. Interfaces *5*, 532–537.
20. Cai, Y., and Tang, R. (2008). Calcium phosphate nanoparticles in biomineralization and biomaterials. J. Mater. Chem. *18*, 3775–3787.
21. Shi, Y., Zhang, Y., Yang, W., and Tang, Y. (2009). Multiradiate calcium phosphate patterns derived from a gradating polysaccharide-acidic protein system. Chem. Commun. 442–444.
22. Rong, H., and Qian, C.X. (2015). Binding functions of microbe cement. Adv. Eng. Mater. *17*, 334–340.
23. Baffoe, E., and Ghahremaninezhad, A. (2022). On the interaction between proteins and cracked cementitious surface. Construct. Build. Mater. *352*, 2.
24. Martin, K., Tirkolaei, H.K., and Kavazanjian, E. (2021). Enhancing the strength of granular material with a modified enzyme-induced carbonate precipitation (EICP) treatment solution. Construct. Build. Mater. *271*, 121529.

25. Müller-Buschbaum, P., Gebhardt, R., Roth, S.V., Metwalli, E., and Doster, W. (2007). Effect of calcium concentration on the structure of casein micelles in thin films. Biophys. J. *93*, 960–968.
26. Rose, D., and Tessier, H. (1959). Effect of various salts on the coagulation of casein. J. Dairy Sci. *42*, 989–997.
27. Frankenberger, W.T., and Johanson, J.B. (1982). Effect of pH on enzyme stability in soils. Soil Biol. Biochem. *14*, 433–437.
28. Khodadadi Tirkolaei, H., Javadi, N., Krishnan, V., Hamdan, N., and Kavazanjian, E. (2020). Crude urease extract for biocementation. J. Mater. Civ. Eng. *32*, 04020374.
29. Schmitz, J.F. (2009). Enzyme Modified Soy Flour Adhesives.
30. Cantaert, B., Kuo, D., Matsumura, S., Nishimura, T., Sakamoto, T., and Kato, T. (2017). Use of amorphous calcium carbonate for the design of new materials. CHEMPLUSCEM *82*, 107–120.
31. Mayer, G. (2005). Rigid biological systems as models for synthetic composites. Science *310*, 1144–1147.
32. Behrens, S.H., and Grier, D.G. (2001). The charge of glass and silica surfaces. J. Chem. Phys. *115*, 6716–6721.
33. De Muynck, W., De Belie, N., and Verstraete, W. (2010). Microbial carbonate precipitation in construction materials: A review. Ecol. Eng. *36*, 118–136.
34. Picker, A., Nicoleau, L., Nonat, A., Labbez, C., and Cölfen, H. (2014). Identification of binding peptides on calcium silicate hydrate: A novel view on cement additives. Adv. Mater. *26*, 1135–1140.
35. Hughes, T.L., Methven, C.M., Jones, T.G., Pelham, S.E., Fletcher, P., and Hall, C. (1995). Determining cement composition by Fourier transform infrared spectroscopy. Adv. Cement Base Mater. *2*, 91–104.
36. Sato, M., and Matsuda, S. (1969). Structure of vaterite and infrared spectra. Z. Kristallogr. N. Cryst. Struct. *129*, 405–410.
37. Gallagher, W. (1997). FTIR Analysis of Protein Structure, pp. 662–666.
38. Yuan, H., Xu, J., Van Dam, E.P., Giubertoni, G., Rezus, Y.L.A., Hammink, R., Bakker, H.J., Zhan, Y., Rowan, A.E., Xing, C., and Kouwer, P.H.J. (2017). Strategies to increase the thermal stability of truly biomimetic hydrogels: Combining hydrophobicity and directed hydrogen bonding. Macromolecules *50*, 9058–9065.
39. Kinsella, J. (1981). Functional properties of proteins: Possible relationships between structure and function in foams. Food Chem. *7*, 273–288.
40. Tas, A.C. (2009). Monodisperse Calcium Carbonate Microtablets Forming at 70°C in Prerefrigerated CaCl2–Gelatin–Urea Solutions. Int. J. Appl. Ceram. Technol. *6*, 53–59.
41. Sheng Han, Y., Hadiko, G., Fuji, M., and Takahashi, M. (2006). Crystallization and transformation of vaterite at controlled pH. J. Cryst. Growth *289*, 269–274.
42. Song, X., Hua, X., Yang, R., Tuo, Y., Wang, S., Wang, J., He, P., and Luo, X. (2023). Synergetic effects of initial NH4+ and Ca2+ concentration on the formation vaterite using steamed ammonia liquid waste as a direct carbonation. Powder Technol. *419*, 118363.
43. Zhou, G.-T., Yao, Q.-Z., Fu, S.-Q., and Guan, Y.-B. (2010). Controlled crystallization of unstable vaterite with distinct morphologies and their polymorphic transition to stable calcite. Eur. J. Mineral. *22*, 259–269.
44. Meldrum, F.C., and Hyde, S.T. (2001). Morphological influence of magnesium and organic additives on the precipitation of calcite. J. Cryst. Growth *231*, 544–558.
45. Lin, Y.P., and Singer, P.C. (2005). Inhibition of calcite crystal growth by polyphosphates. Water Res. *39*, 4835–4843.
46. Bischoff, J.L. (1968). Catalysis, inhibition, and the calcite-aragonite problem; [Part] 2, The vaterite-aragonite transformation. Preprint.
47. Bian, H., and Plank, J. (2012). Re-association behavior of casein submicelles in highly alkaline environments. Z. Naturforsch. Sect. B J. Chem. Sci. *67*, 621–630.
48. Huang, H., Ye, G., and Damidot, D. (2013). Characterization and quantification of self-healing behaviors of microcracks due to further hydration in cement paste. Cement Concr. Res. *52*, 71–81.
49. Baffoe, E., and Ghahremaninezhad, A. (2023). Effect of proteins on the mineralization, microstructure and mechanical properties of carbonation cured calcium silicate. Cem. Concr. Compos. *141*, 105121.
50. Trushina, D.B., Bukreeva, T.V., and Antipina, M.N. (2016). Size-controlled synthesis of vaterite calcium carbonate by the mixing method: Aiming for nanosized particles. Cryst. Growth Des. *16*, 1311–1319.
51. Rodriguez-Navarro, C., Jimenez-Lopez, C., Rodriguez-Navarro, A., Gonzalez-Muñoz, M.T., and Rodriguez-Gallego, M. (2007). Bacterially mediated mineralization of vaterite. Geochem. Cosmochim. Acta *71*, 1197–1213.
52. Njegić-Dzakula, B., Falini, G., Brečević, L., Skoko, Ž., and Kralj, D. (2010). Effects of initial supersaturation on spontaneous precipitation of calcium carbonate in the presence of charged poly-l-amino acids. J. Colloid Interface Sci. *343*, 553–563.
53. Masoule, M.S.T., Baffoe, E., and Ghahremaninezhad, A. (2023). On the physicochemical properties and foaming characteristics of proteins in cement environment. Construct. Build. Mater. *366*, 4.
54. Jagadeesh, D., Jeevan Prasad Reddy, D., and Varada Rajulu, A. (2011). Preparation and properties of biodegradable films from wheat protein isolate. J. Polym. Environ. *19*, 248–253.
55. DeOliveira, D.B., and Laursen, R.A. (1997). Control of calcite crystal morphology by a peptide designed to bind to a specific surface. J. Am. Chem. *119*, 10627–10631.
56. Ye, G., Liu, X., De Schutter, G., Poppe, A.M., and Taerwe, L. (2007). Influence of limestone powder used as filler in SCC on hydration and microstructure of cement pastes. Cem. Concr. Compos. *29*, 94–102.
57. Abd El-Salam, M.H., and El-Shibiny, S. (2016). Natural Biopolymers as Nanocarriers for Bioactive Ingredients Used in Food Industries (Elsevier Inc.).
58. Arriaga, T.V. (2011). Controlled and tailored denaturation and aggregation of whey proteins tatiana vieira arriaga engenharia biológica júri. Thesis.
59. Utay, N.S., Asmuth, D.M., Gharakhanian, S., Contreras, M., Warner, C.D., and Detzel, C.J. (2021). Potential use of serum-derived bovine immunoglobulin/protein isolate for the management of COVID-19. Drug Dev. Res. *82*, 873–879.
60. Znidarsic, W.J., Chen, I.W., and Shastri, V.P. (2009). ζ-potential characterization of collagen and bovine serum albumin modified silica nanoparticles: A comparative study. J. Mater. Sci. *44*, 1374–1380.
61. Barbano, D. (2009). Milk Protein Products - What Are They and What Role Do They Play in Lactose Reduced (Low " Carb ") Foods ? Low " Carb " Dairy Foods and Ingredients . Are Milk Protein Products Safe ? Milk Components and Separation Processes, pp. 1–5.
62. Masoule, M.S.T., Baffoe, E., and Ghahremaninezhad, A. (2023). On the physicochemical properties and foaming characteristics of proteins in cement environment. Construct. Build. Mater. *366*, 130204.
63. Liu, Y., Chen, Y., Huang, X., and Wu, G. (2017). Biomimetic synthesis of calcium carbonate with different morphologies and polymorphs in the presence of bovine serum albumin and soluble starch. Mater. Sci. Eng. C *79*, 457–464.
64. Tunstall, L.E., Scherer, G.W., and Prud'homme, R.K. (2017). Studying AEA interaction in cement systems using tensiometry. Cement Concr. Res. *92*, 29–36.
65. Carmona, J.P.S.F., Venda Oliveira, P.J., Lemos, L.J.L., and Pedro, A.M.G. (2018). Improvement of a sandy soil by enzymatic calcium carbonate precipitation. Proc. Inst. Civ. Eng.: Geotech. Eng. *171*, 3–15.

STAR★METHODS

KEY RESOURCES TABLE

REAGENT or RESOURCE	SOURCE	IDENTIFIER
Chemicals, peptides, and recombinant proteins		
Urease	Sigma Aldrich	Type III Jack Bean Urease
Urea	Sigma Aldrich	CAS: 57-13-6
$CaCl_2$	Sigma Aldrich	CAS: 10043-52-4
Albumin	ONLINESCIENCEMALL	CAS: 9006-59-1
CP	New Zealand	N/A
Whey protein	Premier Research Labs	N/A
NFMP	Prescribed for Life	N/A
SBI	IgG PLus	N/A

RESOURCE AVAILABILITY

Lead contact

Further information and requests for resources should be directed to and will be fulfilled by the lead contact, Ali Ghahremaninezhad (a.ghahremani@miami.edu).

Materials availability

This study did not generate new unique reagents.

Data and code availability

This study did not generate datasets or analyze codes.

METHOD DETAILS

Materials

Proteins

Five proteins with different molecular structures, namely, albumin, collagen peptide (CP), whey protein, non-fat milk powder (NFMP) and sodium immunoglobulin (SBI) were purchased from commercial vendors and used in this study. Albumin comprises about 54-58% of the egg white protein.[57] Whey protein is prepared from the by-product of cheese making.[58] SBI is obtained from edible grade bovine plasma.[59] Collagen peptide constitutes 25-30% of the entire protein composition of the mammals.[60] NFMP is produced by removing moisture from non-fat milk.[61] The molecular structure and physicochemical properties of these proteins have been investigated in our previous study[62] as well as others.[1,10,23,63]

Cement

A type I/II ordinary Portland cement (OPC) was used in the preparation of the cement paste samples. The chemical composition of the type I/II OPC is shown in below table.

Oxide composition of the type I/II ordinary Portland cement used in this study

Oxide	CaO	SiO_2	Al_2O_3	Fe_2O_3	MgO	Na_2O	K_2O	SO_3	LOI	Total
%	64	20.6	4.8	3.5	0.9	0.3	0.1	3.4	2.4	100

Substrate preparation- glass slide and cement paste surface

The binding of EICP and EICP modified with proteins to two surfaces, silica glass slide surface and cement paste surface, was studied. The glass slide had dimensions of 75 mm × 25 mm ×1 mm. Cement paste samples of dimensions of 75 mm × 25 mm × 4 mm with a water/cement of 0.5 were prepared and their surface finely polished at the age of 28 days. The polishing was done using sandpapers of grit sizes 320, 500, and 1200 and finely polished with a 1 μm diamond abrasive paste. The adhesion of precipitates to glass slide surfaces was studied in two

different media with and without 1% concentration of proteins. These media were deionized (DI) water and cement pore solution. The reason for using these different solutions was to investigate the effect of cement chemistry and pH on EICP and EICP adhesion to substrates. The EICP adhesion to cement paste surface was studied in DI water. It should be noted that the surface roughness of the glass slides and finely polished cement paste is different, and this can affect the precipitate binding to the substrate. However, the focus here is on elucidating the effect of the chemistry of the environment on the EICP precipitates and their binding.

Glass slides and finely polished cement paste surfaces were placed horizontally flat in petri dishes. $CaCl_2$ at the concentration of 1.5 M, urea at the concentration of 2 M, and proteins at the concentration of 0% and 1% were added to 50 g of DI water, cement pore solution, and stirred continuously for 10 minutes to ensure complete dissolution. The concentrations of urea and $CaCl_2$ were chosen based on a prior study[1] to yield enough precipitate needed for surface binding and chemical characterization. To prepare the cement pore solution, water was mixed with cement in a ratio of 0.5 and allowed to stand for 30 minutes. The cement pore solution was filtered from the cement mixture using a negative pressure in a filtration setup. The pH of the cement pore solution was measured to be 12.5 using a pH meter. The concentration of Ca^{2+}, Na^{+}, and K^{+} in the cement pore solution is in the range of 2 mM, 90 mM, and 160 mM.[64] The respective solutions were poured into petri dishes containing either glass slide or cement paste. A measure of 250 μL of a 12 kU/L urease concentration was dropped into the solution using a pipette and the petri dishes were covered with a parafilm. A high purity urease enzyme with an activity of 72520 U/g was used in the EICP precipitation. The urease enzyme solution was measured to achieve a concentration of 12 kU/L. 1 U corresponds to the amount of enzyme that hydrolyses 1 μmol of urea per minute at pH 7.0 and 25ºC[65] (Sigma Aldrich Type III Jack Bean Urease). The samples were left to precipitate for 5 days and then the glass slides or cement pastes were removed from the petri dishes and rinsed in DI water for 5 seconds. The samples were then oven-dried and optical images taken of the surfaces.

Material characterization

Scratch test

To investigate the binding strength of the precipitates to the surfaces, a blade of dimension 10 mm × 5 mm × 0.02 mm was used to scratch across the precipitates to investigate their scratch resistances as shown in Figure 1. Images of the surfaces before and after scratching were taken for comparison. The visual deformation or damage left by scratching on the precipitates was used to provide a qualitative measure of binding strength. Some samples showed very small scratch marks while in some others scratching removed a line of the precipitate and exposed the underlying substrate. After the completion of the scratch test, the precipitates were then scraped from the glass slide surface or cement paste surface, ground to a powder and passed through the sieve #60 to be used in FTIR, XRD, TGA, and SEM.

FTIR

FTIR was employed to evaluate the chemical characteristics of the precipitates produced in various conditions. Approximately, 30 mg of the fine EICP powder was utilized in the test. The FTIR measurements were performed using a Perkin Elmer Paragon 1000 FTIR with an ATR accessory (Perkin Elmer, USA) in the transmission mode. The scan resolution was 4 cm^{-1} and spectra were recorded between 600 cm^{-1} and 4000 cm^{-1}. Each sample was taken through 4 scans and an average of two samples from the 4 rounds of scans was reported.

XRD

The XRD analysis of the EICP precipitates was conducted using a Rikagu X-ray Diffractometer (Model D/Max-3C, Rikagu, Japan). The XRD spectra were obtained using the Cu Kα radiation (40 kV, 20 mA) with a scan interval of 2Θ = 10º to 40º, at a step size of 0.02º/s. Approximately 2 g of the fine precipitate powder was loaded into a sample holder, inserted into the device, and scanned. The Rietveld refinement method was used to quantify the relative proportions of the crystalline phases (vaterite, aragonite and calcite) with the Match! phase analysis software.

TGA

Approximately 50 mg of the EICP powder was loaded into the TGA pan. Samples were scanned using the Netzsch TG 209F3 (Netzsch, Germany) at a heating rate of 20°C/min and in the temperature range of 24ºC to 900ºC. Two replicates of each precipitate were used and the average reported.

SEM

The SEM images were obtained using a Zeiss Gemini Ultra Plus FESEM (Zeiss, Germany) in the secondary electron mode. The accelerating voltage was 5 kV at a working distance of 4.5 mm. The magnification of the images was 2.0 kX. The precipitates were gold plated to decrease the effect of charging.